CMT Ceramics in Modern Technologies
Techna Group srl

Properties of Geopolymer Composites from two Different Moroccan Clays

A. El Khomsi[a,b], A. Gharzouni[a], N. Idrissi Kandri[b], A. Zerouale[b] and S. Rossignol[a]*
[a]IRCER, Ecole Nationale Supérieure de Céramique Industrielle, Limoges Cedex, France; [b]Laboratoire de la Chimie Appliquée, Faculté des Sciences et Techniques, Fes, Morocco

The aim of this study is to valorise clays from the Fez region in Morocco as aluminosilicate precursors for geopolymer synthesis. In addition to the clays, the use of calcite and dolomite as mineral additives was also investigated. At first, the Moroccan clays were thermally activated by calcining at 700 °C, and then, a potassium alkaline silicate solution was used for alkali activation. Samples were synthetized by combining clay, metakaolin and mineral additive in several ratios. Consolidated materials were successfully obtained, and geopolymerization reaction was monitored by in situ Fourier transform infrared spectroscopy (FTIR), which revealed several networks. The results demonstrated that composite geopolymers with a mechanical resistance range from 8 to 50 MPa could be obtained from Moroccan clays.

Keywords: Geopolymer, Moroccan clays, Additives, Composite, Mechanical properties.

1. Introduction

Morocco has a wide range of natural resources; among these resources, the clays are particularly diverse and abundant [1]. The extracted clays have been used for years in traditional pottery and bricks and more recently in the manufacture of Portland cement [2]. The main inconveniences of these exploitations are high energy consumption and CO_2 emissions [3]. In recent decades, the international community has shown great concern [4] regarding climate change and environmental pollution, setting aims to eliminate or diminish pollution factors. The Moroccan government has been one of the responsible states that have decided to manage this problem by declaring new laws and restrictions [5]. Recently, local studies have led to innovative applications for clay resources, such as producing low-cost clay-based ultrafiltration membranes [6], removing heavy metals from wastewater by natural clay adsorption, and producing restoration mortar [7] for historical monuments using metakaolin and traditional restoration materials. Most historical monuments were built using lime mortars [8], and this material was used until the First World War. In 1990, a large restoration campaign was undertaken in Europe aiming to conserve historical monuments [9]. After four years, serious deteriorations [9] have been observed, mainly caused by the incompatibility of the restoration materials with the original materials of the old walls; indeed, salt crystallization [10] occurs during the winter in the presence of climatic humidity. Additionally, the utilization of conventional consolidation treatments using synthetic polymers or alkoxysilanes [11] leads to a total failure due to aesthetic, chemical or physico-mechanical incompatibility [12]. Indeed, the penetration of the applied product into the original material is not sufficient; only superficial consolidation occurs, which typically detaches and falls off. The restoration works in Morocco have been carried out using a mixture composed of Portland cement, lime and natural clay taken from nearby monuments to reduce the problems of compatibility. However, the above process is still not sufficient, and some delamination of the new coatings have been observed. Among the materials synthetized at low temperature, alkali-activated and geopolymer materials should be mentioned. These last materials are a new class of binders resulting from the polymerization of aluminium and silicon species in alkaline solution. In 1978, J. Davidovits [13] was the first to introduce the term geopolymers, which result from the dissolution of pure metakaolin in an alkali metal silicate solution. Natural clays containing kaolinite can also be used after thermal activation, which transforms kaolinite to metakaolin. A polymerization of the released aluminium and silicon species forms a three-dimensional amorphous network composed of SiO_4 and AlO_4 tetrahedrons linked by corner-shared oxygen atoms. These materials present many advanced properties, such as good nonflammability [14] and acid resistance [15]; additionally, they have a setting time that can be controlled by the formulation, and are easily shaped [16]. All these characteristics allow numerous industrial applications [17], such as in building materials, nuclear waste holders or military operations [18]. An aluminosilicate source has been the subject of many studies, and it has been demonstrated that raw materials other than metakaolin and natural clays can be used for geopolymer synthesis [19]. In fact, natural clays are heterogeneous; they contain other non-clay-like minerals such as quartz, haematite and carbonates, which can affect the final properties of the geopolymers. Christina K Yip et al [20] highlighted the beneficial effect of a calcite and dolomite addition on the mechanical properties of alkali-activated materials.
The aim of this work is to valorize natural Moroccan clays for potential application with restoration works and for building purposes by using them as aluminosilicate precursors for geopolymer synthesis. To achieve this objective, several

* *Corresponding author*
E-mail address: sylvie.rossignol@unilim.fr

https://doi.org/10.29272/cmt.2020.0001
Received January 3, 2020; Received in revised form February 12, 2020; Accepted February 27, 2020

aluminosilicate precursors and natural Moroccan additives "calcite and dolomite" were used. The obtained consolidated materials were analysed by compressive mechanical tests, TGA analysis and were monitored by in situ FTIR.

2. Experimental Part

2.1. Raw materials and samples preparation

The aluminosilicate precursors used in this work are two Moroccan clays named A1 and A2, in addition to a metakaolin from France called M1. For the additives, calcite and dolomite from Morocco, respectively named CA and DA were used. The clays was grinded at a particle size under 100 μm, using at first a percussion grinder to minimize the grain size to a diameter under 500 μm, then porcelain jars were used to obtain a finer grain size under 100 μm. The grinded clays were calcined at 700 °C for one hour and a half using a heating rate of 28 °C/min in a rotary furnace. The samples preparation was carried out by mixing the calcined clay with KOH pellets (85.2% purity supplied by VWR) previously dissolved in potassium silicate solution (Si/K= 1.7 supplied by ChemLab). Then the reactive mixture was poured into a sealable polystyrene molds, and placed at room temperature (25 °C) to consolidate for seven days, the Figure 1 summarizes the synthesis protocol. The samples are denoted as $A(1 \text{ or } 2)_xM1_yDA(\text{or } CA)_z$, where (A) refers to the calcined Moroccan clay, (M1) to the metakaolin, (CA or DA) to the additives and (x, y and z) to the percentage of each component. For example a sample called $A2_{0.5}M1_{0.5}DA_0$, is composed of 50% of the clay A2, 50% of metakaolin M1 and 0% of the additive DA.

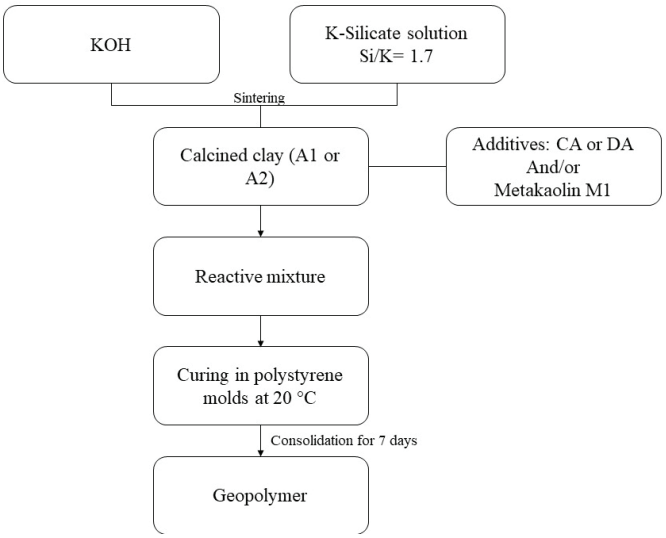

Figure 1. Experimental procedure for the preparation of samples based on the liquid silicate solution and Moroccan raw materials.

2.2. Characterization technics

The chemical composition of the different raw materials was determined by X fluorescence (XRF) using Pnalytical Zetium apparatus, with a photons beam at 1 KW. Acquisitions proceeded from prepared pellets. The preparation was carried out by mixing 1g of the powder to analyze with 10g of (99.5% $Li_2B_4O_7$, 0.5% LiI) then, the mixture were melted at temperature of 1200 °C, and poured in a platinum mold to obtain the pellet.

The specific surface SBET measurements were operated using Micrometric Asap 2020, under N_2 gas at -195.85 °C. The analysis is preceded by the degas of 1g of sample at 200 °C for 9h under vacuum, to ensure that no gas is adsorbed on the surface before the analysis. Then the analysis is operated by adsorption of N_2 gas on the degased sample.

The particle size distribution was measured with a Horiba apparatus, using a laser particle size analyzer. A laser beam cross a glass cell with parallel surfaces, where a suspension of water and the powder is flowing. The analysis is proceeded under ultrasound, to avoid the agglomeration of the particles, to ensure a precise analysis.

The water demand (μL/g) corresponds to the sufficient quantity of water that saturates one gram of powder.

FTIR spectra acquisition were performed on Thermo Fisher Scientific 380 infrared spectrometer (Nicolet), using the attenuated total reflectance (ATR) method. The analysis recording were started at 400 and finished at 4000 cm^{-1}, with a resolution of 4 cm^{-1}. To monitor the geopolymerisation reaction, the software was programed to acquire a spectrum (64 scans) every 10 min for 13 hours. In the post-treatment of the obtained spectra, the CO_2 contribution was removed by a straight-line fit between 2400 and 2280 cm^{-1}, and the baseline were corrected and normalized to permit the comparison.

X-ray diffraction (XRD) patterns were obtained with a Brucker-D8 Advance with a Bragg-Brentano geometry and a Cu Kα_2 detector. The analytical range is between 10_ and 50_ (1 h) with a resolution of 0.02_ (1h) and a dwell time of 1.5 s. Phase identification was performed with reference to a Joint Committee Powder Diffraction Standard (JCPDS). Before analysis, the samples were ground to obtain the powder.

Thermogravitric analysis (TGA) and thermodifferencial analysis (DSC) were performed in Pt crucible between 30 °C and 900 °C using a SDT-Q600. The used ramp is 5 °C/min under a dry airflow of 100 mL/min.

The compressive strength of synthetized materials was evaluated using Instron 5969 testing machine with a crosshead speed of (0.1 mm/min). The samples were aged of 7 days; each composition was tested ten times to obtain an average value. The size of the testing tubes was adjusted to reach a ratio (H/Ø = 2) before the test, using a diamond wheel to obtain a perfect parallel surfaces. The experimental error is obtained from the average of standard deviation.

3. Results and Discussion

3.1. Raw material characterization

The mineralogical composition of the Moroccan raw materials was obtained by XRD analysis; the Table 1 summarizes the obtained results. The clay (A1) is characterized by the presence of kaolinite, quartz, calcite and dolomite, and the second one (A2) is characterized by the same phases in addition to muscovite. On the other hand, the additive CA is essentially composed of calcite,

Table 1. Mineralogical composition of the raw materials A1, A2, CA and DA with the JCPDS files. (K: Kaolinite $[Al_2Si_2O_5(OH)_4]$ (00-006-0221)- Q: quartz $[SiO_2]$ (JCPDS 01-089-1961) - C: calcite $[CaCO_3]$ (00-047-1743) - D: dolomite $[CaMg(CO_3)_2]$ (04-011-9830) - M: muscovite $[K_{0.9}Na_{0.1}Mg_{0.2}Ti_{0.03}Fe_{0.2}Al_{2.4}Si_{3.2}O_{10}(OH)_2]$ (04-011-9830) - I: illite $[K_{0.78}Mg_{0.18}Ti_{0.01}Al_{2.46}Si_{3.36}O_{10}(OH)_2]$ (04-017-0523).

Raw materials	Main mineralogical phases							
	K	I	M	Q	C	D	Pi	Fe
A1	x	-	-	x	x	x	x	X
A2	x	x	x	x	x	x	-	-
CA	-	-	-	x	x	x	-	-
DA	-	-	-	-	x	x	-	-

Table 2. Chemical and physical characteristics of the aluminosilicate sources used.

Physical and chemical characteristics	Aluminosilicate source		Filler	
	A1	A2	CA	DA
Al/Si (molar ratio)	0.33	0.86	0.29	-
Al (mol%)	5.8	6.9	0.6	-
Ca/Si (molar ratio)	0.32	0.38	10	-
D_{50} (μm)	16	9	16	47
S_{bet} (cm^3/g)	46	33	6	2
Water demand (μL/g)	593	665	364	178

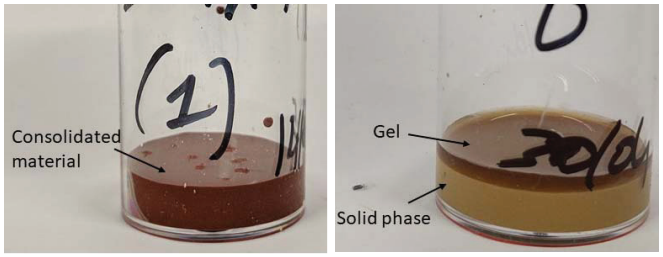

(a) (b)

Figure 2. Photos of the (a) consolidated and (b) unconsolidated materials.

in addition to dolomite and quartz, while the second one DA is essentially composed of dolomite.

The chemical and physical characterizations of each raw material are summarized in the Table 2. The molar ratios for Al/Si are 0.33 and 0.86 for A1 and A2, respectively. However, the molar ratios for Ca/Si are 0.32 for A1 and 0.38 for A2. Consequently, these samples contain a majority of calcium, aluminium and silicon in their composition. The D_{50} values are equal to 16 and 9 μm for the A1 and A2 samples, respectively. The S_{BET} values are equal to 46 and 33 m^2/g for A1 and A2, respectively. Finally, the wettability values are approximately 600 μL/g for both samples. The used additives present particle sizes of 16 and 46 μm for CA and DA, respectively. The weak SBET values (6 and 2 m^2/g) are in agreement with a water demand of 364 and 178 μL/g for CA and DA, respectively.

Commercial metakaolin M1 presents a molar ratio for Al/Si of 0.86 with a specific surface area SBET value of 17 m^2/g [21].

3.2. Feasibility tests

The feasibility of geopolymers based on a mixture of Moroccan clays (denoted A1 or A2), commercial metakaolin (denoted M1), and additives (denoted CA or DA) is investigated. The samples preparation protocol is illustrated in Figure 1; two kinds of morphologies are obtained after 24 hours. One morphology consolidates in a homogeneous state, as shown in Figure 2 (a). The other morphology does not consolidate; instead, it shows two stratified macroscopic phases, which can be observed as a solid precipitate and a floating viscous liquid Figure 2 (b). The ternary diagram A1-M1-CA, as shown in Figure 3 (a), shows two zones corresponding to the consolidated materials (green colour) and unconsolidated materials (red colour). First, it is possible to obtain consolidated material with an (M1-A1) binary. In the presence of A1 clay (A1-CA), the limit of consolidated material reaches 60% Wt of that of A1 calcined clay, up to this value no consolidation occurs, the presence of a gel on the surface of the final material is observed, indicating an excess of siliceous species in the activation solution and a lack of reactive aluminum species from the aluminosilicate source. The same behaviour is

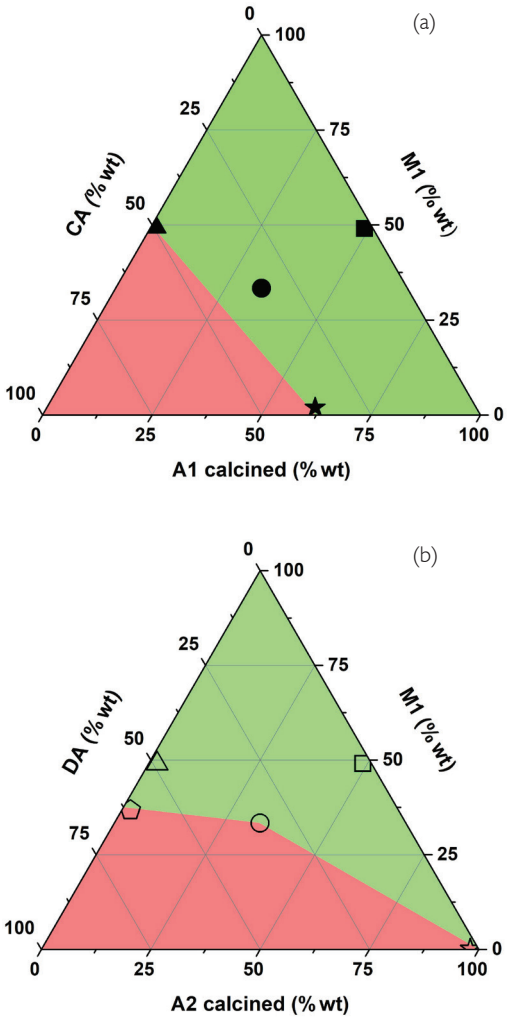

Figure 3. Geopolymer existence domains (a) in the A1-M1-CA ternary zone and (b) in the A2-M1-DA ternary zone, with (—) consolidation zones and (—) unconsolidation zones: (▲) $Al_0M1_{0.5}CA_{0.5}$; (•) $Al_{0.33}M1_{0.33}CA_{0.33}$; (■) $Al_{0.5}M1_{0.5}CA_0$; (★) $Al_{0.63}M1_02CA_{0.37}$; (Δ) $(A2_0M1_{0.5}DA_{0.5})$; (○) $A2_{0.33}M1_{0.33}DA_{0.33}$; (□) $A2_{0.5}M1_{0.5}DA_0$; (☆) $A2_1M1_0DA_0$ and (○) $A2_0M1_{0.37}DA_{0.63}$.

observed in an M1-CA binary, where the limit is 50%. Above this value, no consolidation occurs; indeed, this domain is essentially composed of carbonates that are not reactive, and therefore, induces heterogeneity in the final material. All these limits allow us to determine the domain of existence in the ternary. The changes in the clay and the additive induce different behaviours, for instance, A2-M1-DA, as shown in Figure 3 (b). It is always possible to obtain consolidated materials in (A2-M1) and DA-M1 binaries, however for the last one the limit (60 % Wt) is slightly superior compared to (CA-M1). In (A2-DA) binary consolidation occurs only when A2 clay is used alone, but the addition of CA do not allow consolidation. Indeed, this clay contains few kaolinite affecting the available aluminium species able to react and conduct to geopolymerisation reaction. In addition to that, the other minerals such as muscovite and illite do not react with the activation solution, which can explain the low reactivity of this clay.

It is important to mention that the quantity of raw materials used in the first ternary A1-M1-CA is superior to that used in A2-M1-DA with respect to the water demand of the raw materials, as cited in Table 3. These results indicate that the studied Moroccan clays allow the formation of consolidated material, either in its calcined pure form, which is the case of A1 and A2, or in a mixed form with the additives and metakaolin. The different behaviours observed in the ternaries are directly linked with the nature of

Moroccan clays. But improving the content of metakaolin appears as a way to use these clays in another domains.
The following steps of this work will focus on three formulations based on A1-M1-CA [$A1_0M1_{0.5}CA_{0.5}$; $A1_{0.33}M1_{0.33}CA_{0.33}$ and $A1_{0.5}M1_{0.5}CA_0$] and three other formulations based on A2-M1-DA [$A2_0M1_{0.5}DA_{0.5}$; $A2_{0.33}M1_{0.33}DA_{0.33}$ and $A2_{0.5}M1_{0.5}DA0$], with the aim of understanding the different parameters that govern geopolymerization.

Table 3. Weight loss values obtained from the TGA curves of the studied samples after ageing for 7 days.

	Sample	Wt. loss (%wt) 30-250 °C	Wt. loss (%wt) 250-600 °C	Wt. loss (%wt) 600-900 °C
A1	$A1_0M1_{0.5}CA_{0.5}$	23	2	12
	$A1_{0.33}M1_{0.33}CA_{0.33}$	24	2	8
	$A1_{0.5}M1_{0.5}CA_0$	22	1.5	1
A2	$A2_0M1_{0.5}DA_{0.5}$	28	2	12
	$A2_{0.33}M1_{0.33}DA_{0.33}$	27.5	2.5	9
	$A2_{0.5}M1_{0.5}DA_0$	26.5	2	3

3.3. Effect of A1 and A2 clay on the polycondensation reaction

An FTIR analysis was performed on the six studied formulations based on A1 clay ($A1_0M1_{0.5}CA_{0.5}$; $A1_{0.33}M1_{0.33}CA_{0.33}$ and $A1_{0.5}M1_{0.5}CA_0$) and on A2 clay ($A2_0M1_{0.5}DA_{0.5}$; $A2_{0.3}3M1_{0.33}DA_{0.33}$ and $A2_{0.5}M1_{0.5}DA_0$). The FTIR spectra obtained at t = 0 min and t = 400 min are reported in Figure 4.
Sample $A1_0M1_{0.5}CA_{0.5}$ shows the presence of a large peak at approximately 3400 cm^{-1} at the beginning of the reaction, which is associated with -OH stretching, and a sharp peak at 1620 cm^{-1}, which can be attributed to the –OH bending of water [22]. Carbonate species are observable at approximately 1430 cm^{-1}

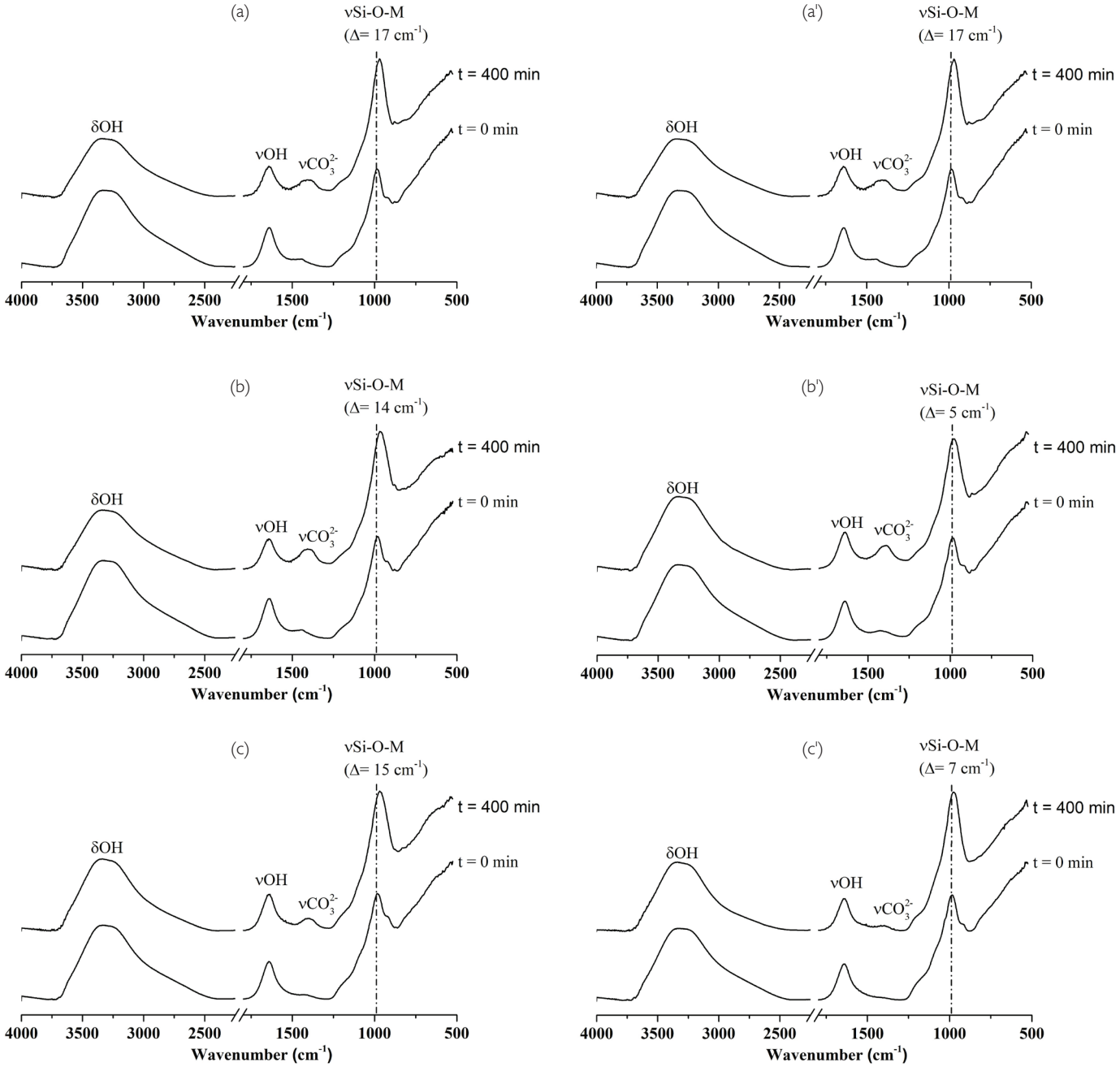

Figure 4. In situ FTIR spectra obtained at t = 0 and after 400 min for the (a) $A1_0M1_{0.5}CA_{0.5}$; (b) $A1_{0.33}M1_{0.33}CA_{0.33}$; (c) $A1_{0.5}M1_{0.5}CA_0$; (a') $A2_0M1_{0.5}DA_{0.5}$; (b') $A2_{0.33}M1_{0.33}DA_{0.33}$ and (c') $A2_{0.5}M1_{0.5}DA_0$ samples (Δ= Shift of the Si-O-M band).

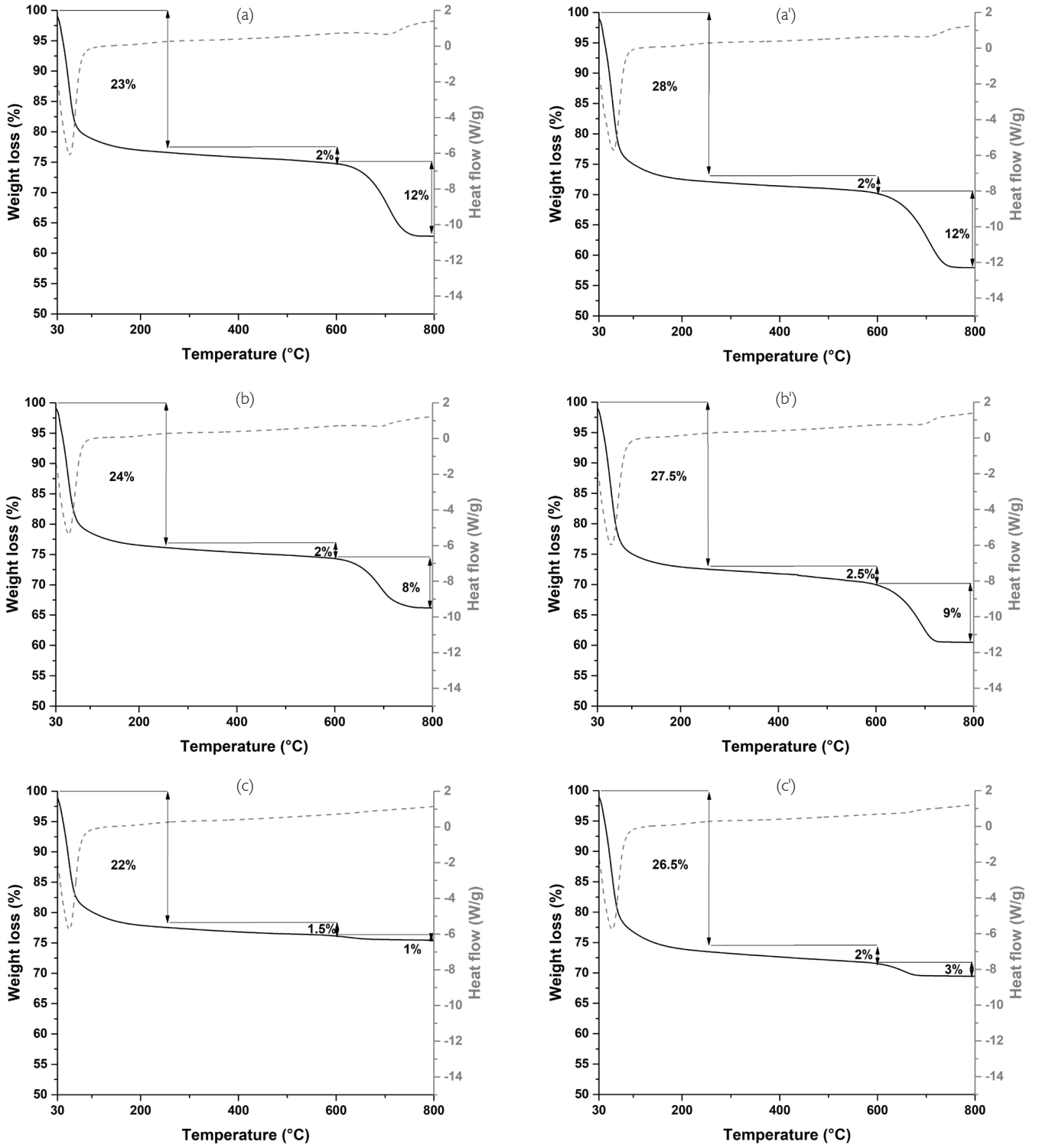

Figure 5. Thermal analysis curves of (a) $A1_0M1_{0.5}CA_{0.5}$; (b) $A1_{0.33}M1_{0.33}CA_{0.33}$; (c) $A1_{0.5}M1_{0.5}CA_0$; (a') $A2_0M1_{0.5}DA_{0.5}$; (b') $A2_{0.33}M1_{0.33}DA_{0.33}$ and (c') $A2_{0.5}M1_{0.5}DA_0$ samples.

[23]. At approximately 980 cm^{-1}, an intense and large bond is observed, which is attributed to Si-O-M (M = Si, Al...) [24]. After 400 min, several structural changes are noted. The intensity of the water peaks at 3400 and 1620 cm^{-1} diminish, indicating the consumption of water by a polycondensation reaction. The carbonate peak intensity increases, in addition to a slight change in their position (1387 cm^{-1}), which is caused by the formation of potassium carbonates (K_2CO_3) [25]. A shift to lower wavenumbers is observed for the Si-O-M bond (Δ=17 cm^{-1}), which is induced by the substitution of silicon atoms with aluminium atoms, indicating that a polycondensation reaction occurs, which has been previously evidenced by several authors [26,27]. The addition of A1 clay ($A1_{0.33}M1_{0.33}CA_{0.33}$ and $A1_{0.5}M1_{0.5}CA_0$), as shown in Figure 4 (a) and Figure 4 (b), induces a decrease in the shift, with values of 5 and 7 cm^{-1}, respectively. This may be due to the change in the aluminosilicate source. In this case, the available aluminium content changes, and consequently, the formed networks are different [28]. The formulations containing A2 clay display the same shift values of approximately 15 cm^{-1}. All these data demonstrate that some polycondensation occurs in these consolidated materials, and an explanation will be given in the discussion section.

To evaluate the water content in these consolidated materials, thermal analysis was performed. Figure 5 regroups the obtained

thermogravimetric curves for each studied formulation. The weight loss values are gathered in Table 3. Similar behaviour is obtained. As an example, for the $A1_0M1_{0.5}CA_{0.5}$ sample Figure 5 a, the first endothermic peak shows a weight loss of 23% from 30-250 °C, which is associated with the departure of the free and adsorbed water [29]. A slight weight loss of 2% between 250 and 600 °C may be due to some hydroxyl groups of residual kaolinite remaining from the calcination process [30]. After 600 °C, a weight loss of 12% is caused by the decomposition of the carbonate species in CA. For the $A1_{0.33}M1_{0.33}CA_{0.33}$ and $A1_{0.5}M1_{0.5}CA_0$ samples, the same behaviour is observed with a small weight loss in the range of 600-900 °C due to a minor amount of carbonates. The same phenomenon occurs for the A2 clay samples. This observation confirms that a calcination temperature of 700 °C does not totally decompose the carbonates that are present in the clays. However, the water content due to the polycondensation remains higher for A2 (28%) clays in comparison to A1 clays, which can be attributed to the weak reactivity of the A2 system.

Compressive tests were carried out on the six studied samples, which permitted us to evaluate their mechanical resistance (Figure 7, Table 4). The curves related to the $A1_0M1_{0,5}CA_{0,5}$ sample present the behaviour of a fragile material with a maximum

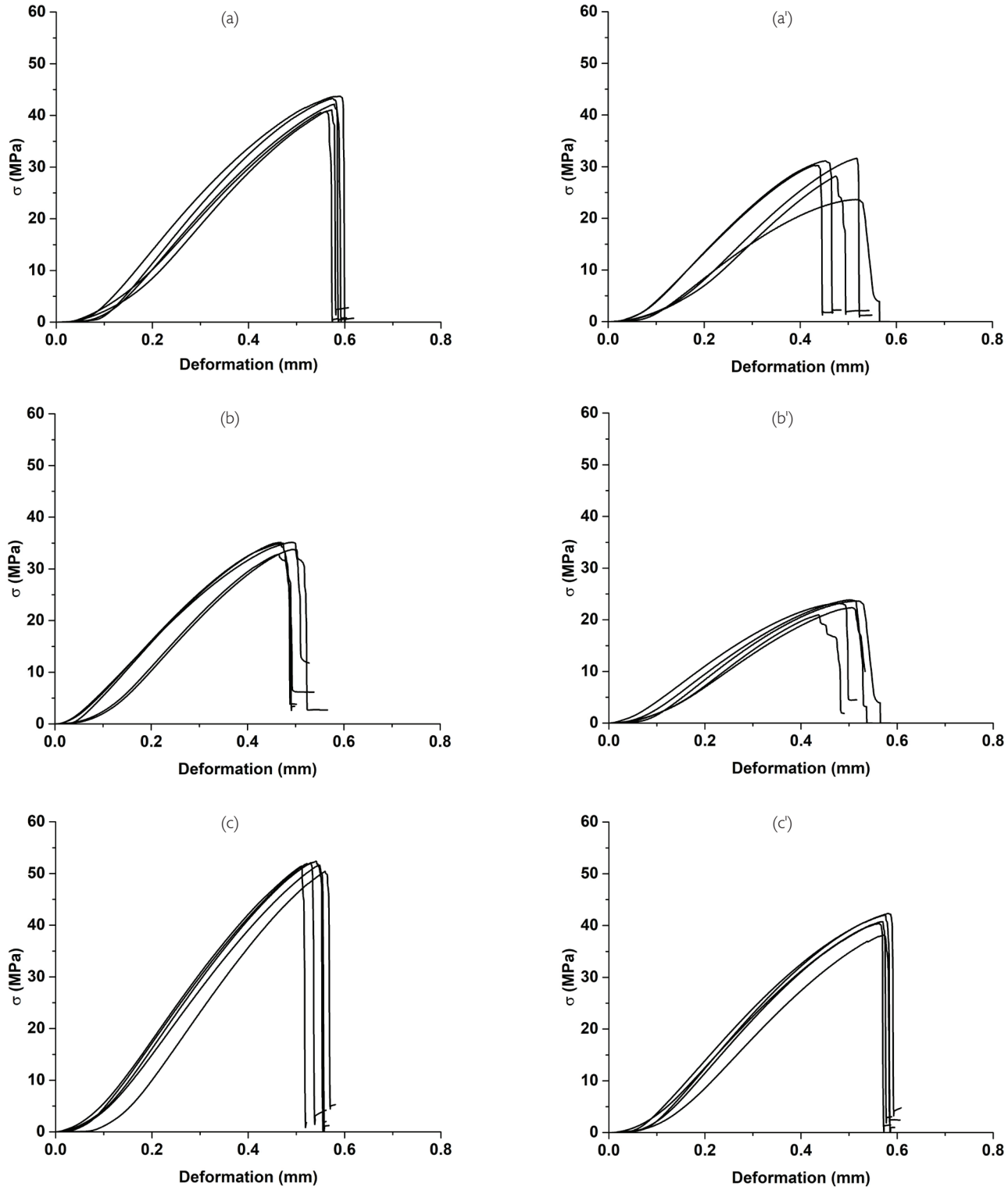

Figure 6. Compressive strength curves of the (a) $A1_0M1_{0.5}CA_{0.5}$; (b) $A1_{0.33}M1_{0.33}CA_{0.33}$; (c) $A1_{0.5}M1_{0.5}CA_0$; (a') $A2_0M1_{0.5}DA_{0.5}$; (b') $A2_{0.33}M1_{0.33}DA_{0.33}$ and (c') $A2_{0.5}M1_{0.5}DA_0$ samples.

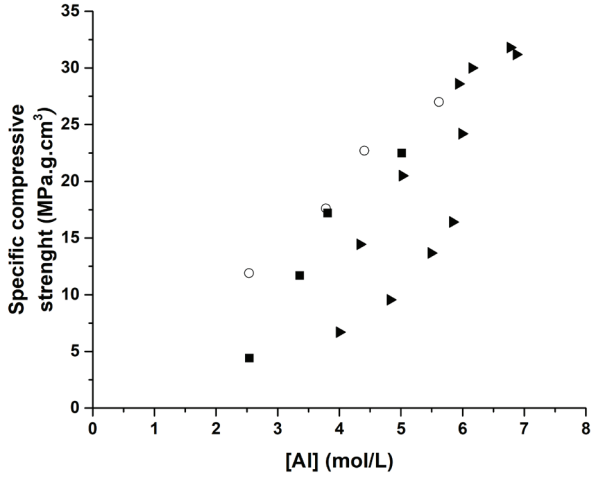

Figure 7. Compressive strength plotted as a function of the aluminium concentration: (○) A1-based materials, (■) A2-based materials (▶), and M1- or argillite-based materials.

Table 4. Average values of compressive strength and physicochemical properties of the studied consolidated materials.

	Formula	σ (±2 MPa)	Si/Al	[Al] (mol/L)
A1	$A1_0M1_{0.5}CA_{0.5}$	42	1.52	4.4
	$A1_{0.33}M1_{0.33}CA_{0.33}$	33	1.98	3.8
	$A1_{0.5}M1_{0.5}CA_0$	50	1.84	5.6
A2	$A2_0M1_{0.5}DA_{0.5}$	31	1.63	3.8
	$A2_{0.33}M1_{0.33}DA_{0.33}$	21	2.05	3.4
	$A2_{0.5}M1_{0.5}DA_0$	40	1.87	5.0

resistance of 42 MPa. The addition of A1 clay ($A1_{0.33}M1_{0.33}CA_{0.33}$) induces a decrease to 33 MPa. Without additive ($A1_{0.5}M1_{0.5}CA_0$), a maximum compressive strength is reached with the same behaviour. A change from A1 clay to A2 clay induces a decrease in the compressive strength values, and the behaviour becomes similar to that of a composite. This can be explained by the difference in the clay mineralogy between the A1 and A2 samples discussed in the following section.

4. Discussion

The synthetized samples show various behaviours depending on the formulation, especially when considering the type of clay and the metakaolin content. The observed shifts depend on the raw material that is used; indeed, the highest shift values are registered for samples based on A2 clay. This fact indicates the presence of several networks resulting from the dissolved metakaolin phase and the impurities released from the natural clay. In contrast, the use of A1 clay induces low shifts, suggesting the presence of less impurities in the clay and a more developed geopolymer network in the final material. To validate this behaviour, the water content values (TGA analysis) are gathered in Table 3. The data reveal that A1-based samples exhibit less water content than A2-based samples. Gharzouni et al [31] demonstrated that a low water content indicated good reactivity based on "water consumption during the polycondensation reaction" and a well-developed geopolymer network. These observations corroborate with the FTIR results, where it is evidenced that the A1 clay (low shift) is more reactive than the A2 clay. It should be taken into consideration that A1-based materials contain a higher quantity of solid precursors compared to that of A2-based samples, which also contributes to water consumption (availability of more reactive species). Based on this information, the reactivity of the A1 clay seems to be higher than that of A2. Moreover, it is important to take into consideration the fact that A1-based samples contain a notable amount of aluminosilicate precursor, which provides more reactive aluminium.

Since all the compositions studied are based on metakaolin, clay and additive, the compressive strength values are plotted as a function of the aluminium concentration in Figure 8. For comparison, data corresponding to materials based on metakaolin with and without additives [32] and coproduct-based materials [33] are added. As a reference for comparison, pure metakaolin-based materials exhibit a proportional variation of the mechanical strength versus the aluminium concentration; thus, samples that are rich in aluminium present a high resistance (σ_{max} = 32 MPa.cm^3/g). The addition of mineral filler leads to similar mechanical properties as the pure metakaolin-based samples. On the other hand, the use of natural coproducts results in low mechanical strength, unless the aluminium concentration is high. The Moroccan clay-based materials follow the same trend as the reference samples; however, the mechanical resistances are weaker. It is well known in the literature that the availability of dissolved aluminium species allows the formation of a geopolymer network that provides high mechanical strength[33]. Indeed, the samples poor in aluminium, such as the $A2_1M1_0DA_0$ sample, show a low compressive strength (5 MPa.cm^3/g), while mixed formulations containing metakaolin and Moroccan clay exhibit resistance similar to those of the reference samples, such as $A1_{0.5}M1_{0.5}CA_0$ (27 MPa.cm^3/g). Moreover, the Moroccan clays contain associated minerals such as quartz, illite and smectites, which means that a part of the aluminium contained in natural clays is unreactive. Consequently, these materials can be similar to composite geopolymers since the clays act as both reactive and unreactive clays. These data highlight the relationship between the chemical composition of the clays and the final properties of the geopolymers.

5. Conclusion

The aim of this work is to use Moroccan raw materials such as clay and mineral additives for formulating geopolymers. The main results are as follows:

- Formulations based on Moroccan raw materials calcined at 700 °C allow us to obtain geopolymer materials, which are evidenced by FTIR data displaying the formation of several networks.
- The obtained materials exhibit satisfying mechanical strength values, varying from 8 to 50 MPa, depending on the type and amount of clay, metakaolin and additive used in the formulation.
- In addition, the relationship between the chemical composition and final mechanical properties of the consolidated samples show that these materials behave as several geopolymers and composites, correlating that the various impurities are able to produce geopolymer composites.

From this perspective, the suitability of the developed materials for historical monument restoration will be tested to evaluate the compatibility between the original stones and the restoration mortar.

References

[1] P. Billaux, G. Bryssine, Les sols du Maroc. In : Congrès de pédologie méditerranéenne : excursion au Maroc. Cahiers de la Recherche Agronomique, 1 (24), 59-101. Congrès de Pédologie Méditerranéenne, Madrid (ES), 1966.

[2] S. Fellaou, T. Bounahmidi, Evaluation of energy efficiency opportunities of a typical Moroccan cement plant: Part I.

Energy analysis, Appl. Therm. Eng., vol. 115, p. 1161- 1172, 2017.
[3] Y. Li, al., Environmental impact analysis of blast furnace slag applied to ordinary Portland cement production, J. Clean. Prod., vol. 120, p. 221- 230, 2016.
[4] J. Véron, III. La communauté internationale, l'environnement, le développement et la population, In Jacques Véron (eds.), Démographie et écologie. La Découverte, p. 43- 52, 2013.
[5] S. Idllalène, La Charte marocaine de l'Environnement et du Développement durable sera-t-elle une loi fondamentale ?, VertigO - Rev. Électronique En Sci. Environ., 2010.
[6] H. Ouaddari, A. Karima, B. Achioua, S. Sajaa, A. addanea, J. Bennazha, I. El Amrani El Hassani, M. Ouammou, A. Albizane, New low-cost ultrafiltration membrane made from purified natural clays for direct Red 80 dyeremoval, J. Environ. Chem. Eng., vol. 7, no 4, p. 103268, 2019.
[7] F. Allali, E. Joussein, N. I. Kandri, S. Rossignol, The influence of calcium content on the performance of metakaolin-based geomaterials applied in mortars restoration, Mater. Des., vol. 103, p. 1- 9, 2016.
[8] S.-H. Kang, S.-O. Lee, S.-G. Hong, Y.-H. Kwon, Historical and scientific investigations into the use of hydraulic lime in Korea and preventive conservation of historic masonry structures, Sustain. Switz., 11, no 19.
[9] P. De Brandois, F. Babics, Manuel de sensibilisation à la restauration de la maçonnerie. Ministère de la culture et de la communication, Direction de l'architecture et du patrimoine, 2006.
[10] A. Klisinska-Kopacz, R. Tišlova, The Effect of Composition of Roman Cement Repair Mortars on Their Salt Crystallization Resistance and Adhesion, Procedia Eng., vol. 57, p. 565-571. 2013.
[11] K. Elert, E.S. Pardo, C. Rodriguez-Navarro, Alkaline activation as an alternative method for the consolidation of earthen architecture, J. Cult. Herit., vol. 16, no 4, p. 461- 469, 2015.
[12] R. Snethlage, K. Sterflinger, Stone Conservation, in Stone in Architecture: Properties, Durability, S. Siegesmund, R. Snethlage, Éd. Berlin, Heidelberg: Springer Berlin Heidelberg, 2011, p. 411- 544.
[13] J. Davidovits, Geopolymers and geopolymeric materials, J. Therm. Anal., vol. 35, no 2, p. 429- 441, 1989.
[14] S. K. Saxena, M. Kumar, N. B. Singh, Fire Resistant Properties of Alumino Silicate Geopolymer cement Mortars, Mater. Today Proc., vol. 4, no 4, Part E, p. 5605- 5612, 2017.
[15] T. Bakharev, Resistance of geopolymer materials to acid attack, Cem. Concr. Res., vol. 35, no 4, p. 658- 670. 2005.
[16] Y.-S. Wang, Y. Alrefaei, J.-G. Dai, Silico-Aluminophosphate and Alkali-Aluminosilicate Geopolymers: A Comparative Review, Front. Mater., 6, 2019.
[17] H. Xu, J. S. J. Van Deventer, The geopolymerisation of alumino-silicate minerals, Int. J. Miner. Process., vol. 59, no 3, p. 247- 266, 2000.
[18] P.G. Malone, T. Kirkpatrick, C.A. Randall, Potential applications of alkali-activated alumino-silicate binders in military operations, Report WES/MP/GL-85-15, US Army, Corps of Engineers, Vicksburg, MS, 1986.
[19] H. Xu, J. S. J. Van Deventer, Geopolymerisation of multiple minerals, Miner. Eng., vol. 15, no 12, p. 1131- 1139, 2002.
[20] K. Yip Christina, J. L. Provis, G.C.L. Jannie, J.S.J. Van Deventer, Carbonate mineral addition to metakaolinbased geopolymers. Cement&Concrete Composites, 2008, 30, p.979-985.
[21] A. Gharzouni (2016), Contrôle de l'attaque des sources aluminosilicates par la compréhension des solutions alcalines. Thesis, dept. ceramic proceeding and surface treatment; Limoges university, France.
[22] G. Socrates, Infrared and Raman Characteristic Group Frequencies: Tables and Charts, George Socrates John Wiley and Sons, Ltd, Chichester, Third Edition, 2001.
[23] S. Gunasekaran, G. Anbalagan, S. Pandi, Raman and infrared spectra of carbonates of calcite structure, J. Raman Spectrosc., 37, no 9, p. 892- 899, 2006.
[24] E. Prud'homme, P. Michaud, E. Joussein, J.-M. Clacens, S. Rossignol, Role of alkaline cations and water content on geomaterial foams: Monitoring during formation, J. Non-Cryst. Solids, vol. 357, no 4, p. 1270- 1278, 2011.
[25] C.K. Huang, P. F. Kerr, Infrared study of the carbonate minerals, Am. Mineral., vol. 45, no 3- 4, p. 311- 324, 1960.
[26] A. Gharzouni, E. Joussein, B. Samet, S. Baklouti, S. Rossignol, Effect of the reactivity of alkaline solution and metakaolin on geopolymer formation, J. Non-Cryst. Solids, 410, p. 127-134, 2015.
[27] P. Duxson, J.L. Provis, Designing Precursors for Geopolymer Cements, J. Am. Ceram. Soc., vol. 91, no 12, p. 3864- 3869, 2008.
[28] N. Belmokhtar, H. El Ayadi, M. Ammari, L. Ben Allal, Effect of structural and textural properties of a ceramic industrial sludge and kaolin on the hardened geopolymer properties, Appl. Clay Sci., 162, p. 1-9, 2018
[29] D.S. Perera, E. R.Vance, K.S. Finnie, M.G. Blackford, J.V. Hanna, D.J. Cassidy,C.L. Nicholson, Disposition of water in metakaolinite-based geopolymers, Ceram.Trans. 185 (2005) 225-236.
[30] E. Gasparini, E. Serena, C. Tarantino, P. Ghigna, M. Pia Riccardi, E. Cedillo-González c, C. Siligardi, M. Zema, Thermal dehydroxylation of kaolinite under isothermal conditions, Appl. Clay Sci., vol. 80- 81, p. 417- 425, 2013
[31] A. Gharzouni, E. Joussein, B. Samet, S. Baklouti, S. Rossignol, Effect of the reactivity of alkaline solution and metakaolin on geopolymer formation, J. Non-Cryst. Solids, 410, p. 127-134, 2015.
[32] A. Gharzouni, L. Vidal, N. Essaidi, E. Joussein, S. Rossignol, Recycling of geopolymer waste: Influence on geopolymer formation and mechanical properties, Mater. Des., 94, p. 221- 229, 2016.
[33] C. Dupuy, A. Gharzouni, N. Texier-Mandoki, X. Bourbon, S. Rossignol, Alkali-activated materials based on callovo-oxfordian argillite: Formation, structure and mechanical properties, J. Ceram. Sci. Technol., 9, no 2, p. 127- 140, 2018.